https://doi.org/10.5194/essd-2026-490
Preprint. Discussion started: 11 August 2026

Open Access Earth System Science Data Discussions

Thirteen years of aerosol chemical composition measurements in the Paris region: reprocessing and applications

Juliette Brochet[1,2], Hasna Chebaicheb[3,2], Olivier Favez[3,2], Laura Cadeo[4], Tanguy Amodeo[3], Yunjiang Zhang[5], Antonin Bergé[1,2], Philip Croteau[6], Vincent Crenn[7], Valérie Gros[1], and Jean-Eudes Petit[1,2]

[1]Laboratoire des Sciences du Climat et de l'Environnement (LSCE), CEA, CNRS, UVSQ, Université Paris-Saclay, Gif-sur-Yvette, France
[2]Aerosol Chemical Monitor Calibration Centre (ACMCC), CEA/Orme des Merisiers, Gif-sur-Yvette, France
[3]Institut National de l'Environnement Industriel et des Risques (INERIS), Verneuil-en-Halatte, France
[4]University of Milan, Milan, Italy
[5]Nanjing University of Information Science and Technology (NUIST), Nanjing, Jiangsu, China
[6]Aerodyne Research, Inc, Billerica, Massachusetts, USA
[7]ADDAIR, Buc, France

Correspondence: Jean-Eudes Petit (jean-eudes.petit@lsce.ipsl.fr)

Abstract. The recent development of very long-term Aerosol Chemical Speciation Monitor (ACSM) time series presents new insights into the spatiotemporal variability of atmospheric submicron aerosol (PM_1) composition. However, challenges in analyzing long-term datasets remain due to their discontinuities. This study proposes a new methodology to homogenize long-term features monitored at the semi-urban SIRTA observatory, located in the Paris region, and then analyzes the variability of the reprocessed dataset, which can be found in EBAS database at https://doi.org/10.48597/4RKH-6RDU (Petit, J.-E. and Brochet, J. and ACTRIS and GAW-WDCA, 2025). Response factor (RF) and relative ionization efficiencies (RIEs) have been identified as major parameters to reevaluate, as the concentrations of aerosol are most sensitive to these parameters. Secondly, corrections of ion transmission and mass calibration present a smaller, yet significant, interest in the harmonization protocol. This approach shows a good consistency with the latest standard operation protocol and encouraging results when compared to previous studies. Long-term datasets allow the evaluation of parameterizations like the composition-dependent collection efficiency (CDCE) determined by Middlebrook et al. (2012). In this case, the SIRTA dataset shows a good correlation with the CDCE equations, as they stay in its data inter-quartile range, despite the lack of extreme concentration values recorded at the SIRTA observatory. However, this study shows better data consistency with a default collection efficiency (CE) of 0.5 rather than 0.45.

From 2012 to 2024, PM_1 have decreased by 3 $\mu g/m^3$/yr. Within PM_1 components, NH_4 and SO_4 are significantly decreasing at the annual and seasonal scale, in Autumn (NH_4 -0.050 and -0.053 $\mu g/m^3$/yr, SO_4 -0.044 and -0.046 $\mu g/m^3$/yr respectively). Spring, with the highest PM_1 concentrations, demonstrates significant decreasing trends for the majority of PM_1 components (OM -0.21 $\mu g/m^3$/yr, NO_3 -0.23 $\mu g/m^3$/yr, NH_4 -0.12 $\mu g/m^3$/yr and SO_4 -0.093 $\mu g/m^3$/yr). Compared with the original dataset, these results highlight the critical importance of harmonized reprocessing for the analysis of very long-term features. Persistent Pollution Episodes (PPE) also have a decreasing trend of occurrence (5 % per year) and might correlate between their duration

https://doi.org/10.5194/essd-2026-490
Preprint. Discussion started: 11 August 2026

Open Access Earth System Science Data Discussions

and maximum concentrations. These trends are placed in the context of synoptic weather regimes, in which blocking regimes dominate the formation of PPE. Finally, the long-term measurements of SO_4 at SIRTA reveal the need for S-related source apportionment analysis, through the identification of the contributions of volcanic and marine biogenic aerosols. Overall, with the general reduction in atmospheric aerosol concentrations, this study shows encouraging results for air quality, emphasizing the need to maintain mitigation efforts in the Paris region.

1 Introduction

Atmospheric aerosol pollution has been considered over the years as a major challenge, due to its deleterious impacts on both human health and climate (Beelen et al. (2014); Li et al. (2022)). Indeed, atmospheric aerosols can affect the respiratory and cardiovascular systems, depending notably on their chemical composition and size. The European Environment Agency recently stated that 239,000 premature deaths were attributable to $PM_{2.5}$ in 2022 in Europe (European Environment Agency, 2024). Latest air quality guidelines from the World Health Organization (WHO, 2021) set an annual mean limit value of $PM_{2.5}$ at 5 $\mu g/m^3$. However, this recommendation is often exceeded in most urban areas worldwide (Lolli, 2025), exacerbating the sanitary impacts of atmospheric pollution due to high population density. On the other hand, atmospheric aerosols can be associated with a deterioration of visibility, through the formation of pollution episodes, either dominated by primary (e.g., Foret et al. (2022)) or secondary material (Huang et al. (2025); Patel et al. (2021)). Upon composition, they can also have a cooling or warming effect on the climate system, depending on their radiative properties (Szopa et al., 2023).

As a response, the chemical composition of aerosols has been characterized for decades, highlighting the variety of sources, transformation processes under different meteorological conditions, and the wide range of components and concentrations (Fomba et al. (2014); Zhang et al. (2014); Klopper et al. (2020)). Measurements based on filter samplings and subsequent chemical analyses can suffer from poor temporal resolution, high operating costs and delay between sampling and results. For this purpose, aerosol mass spectrometers (Jayne et al., 2000) and more specifically Aerosol Chemical Speciation Monitors (ACSMs, Ng et al. (2011)) have been able to provide robust information on the chemical composition of non-refractory components of submicron aerosols ($NRPM_1$) since 2011. Multi-year datasets (1-2 years) are now rather legion, especially in Europe (Chen et al., 2022), but also at other locations worldwide (Zhou et al., 2020), enhancing our understanding of the determinants of their spatiotemporal variability (e.g., Bressi et al. (2021)). The pooling of multiple datasets, as promoted by networks and research infrastructures such as ASCENT and ACTRIS, can further enable a comprehensive glance at seasonality, model performance (Tsimpidi et al., 2025), and geographical origins (Schneider et al., 2025). Additionally, from subsequent source apportionment analysis, ACSM measurements can provide meaningful information on the different fractions of organic aerosols (OA, e.g., Chen et al. (2022)), and for instance, the impacts of brutal policy changes on the sources of OA (e.g., Petit et al. (2021); Chen et al. (2025)).

Nevertheless, a robust characterization of long-term trends, which would enable a critical evaluation of mitigation policies as well as epidemiological studies, requires more than 10 years of continuous measurements. By contrast, very long-term ACSM measurements (more than 10 years) are still scarcely reported (Atabakhsh et al., 2025), which can be linked to the

https://doi.org/10.5194/essd-2026-490
Preprint. Discussion started: 11 August 2026

relative youth of the ACSM technology and the level of effort required to operate, maintain, and process these kinds of data. Moreover, a 10+ year time series can often result from the juxtaposition of separate data processing periods over the years. Adding the evolution of operators, instrument's knowledge, calibration protocols, and data processing, as well as different breakdowns and maintenance, discontinuities appear within the dataset, which can make it inconsistent between different periods. This heterogeneity may prevent a robust and relevant analysis of long-term features. Therefore, a dedicated strategy for data processing must be developed in order to address these unanticipated challenges.

In this context, the present paper documents ACSM measurements carried out since 2011 at the SIRTA observatory, located in the Paris region, France. Based on this unique dataset, we propose a data reprocessing strategy that yields the first homogeneous, longest ACSM timeseries worldwide. Then, we demonstrate how calibration and correction parameters can be optimized to strike a balance between the dataset homogeneity and the instrument's operation. The length of the dataset also allows for evaluating data corrections that have a significant impact on concentrations, such as the Composition Dependent Collection Efficiency (CDCE; Middlebrook et al. (2012)). Finally, we showcase some of the long-term features of the dataset, such as trends, and how they can relate to mitigation policies, as well as specific pollution episodes in the Paris region and trajectory analysis of sulfated particles.

2 Material and methods

2.1 Sampling site

The SIRTA observatory (Site Instrumental de Recherche par Télédétection Atmosphérique, http://sirta.ipsl.fr) is a suburban site located 20 km south-west of Paris. It is one of the ACTRIS national facilities, where trace gases and aerosol loadings have been continuously characterized for more than a decade. Thanks to its location, SIRTA provides a good representation of the urban background pollution of the Paris region (Haeffelin et al., 2005). In this context, aerosol in situ measurements have been carried out since 2011, with different instrumentations described below.

In particular, the same Q-ACSM has been measuring the composition of PM_1 since 2011 and continues to do so today. This instrument now serves as a reference for others, as is the case during the Aerosol Chemical Monitor Calibration Center (ACMCC) annual intercomparison campaign. The ACMCC is an ACTRIS facility within the Center for Aerosol In-Situ - European Center for Aerosol Calibration and Characterization (CAIS-ECAC), which ensures the good operation of aerosol chemical monitors and the quality of their measurements. Thanks to the mission of the ACMCC to improve standard operation protocol, the SIRTA Q-ACSM has followed the latest guidelines and has been regularly calibrated for more than thirteen years, making it a good candidate for the development of a long-term dataset reprocessing method.

2.2 Measurement principles of the Aerosol chemical speciation monitor

Q-ACSMs enable the characterization of atmospheric non-refractory components according to the following principle. The air is sampled through a switching valve, alternating between two modes. Sample mode lets particles and gases through, while

https://doi.org/10.5194/essd-2026-490
Preprint. Discussion started: 11 August 2026

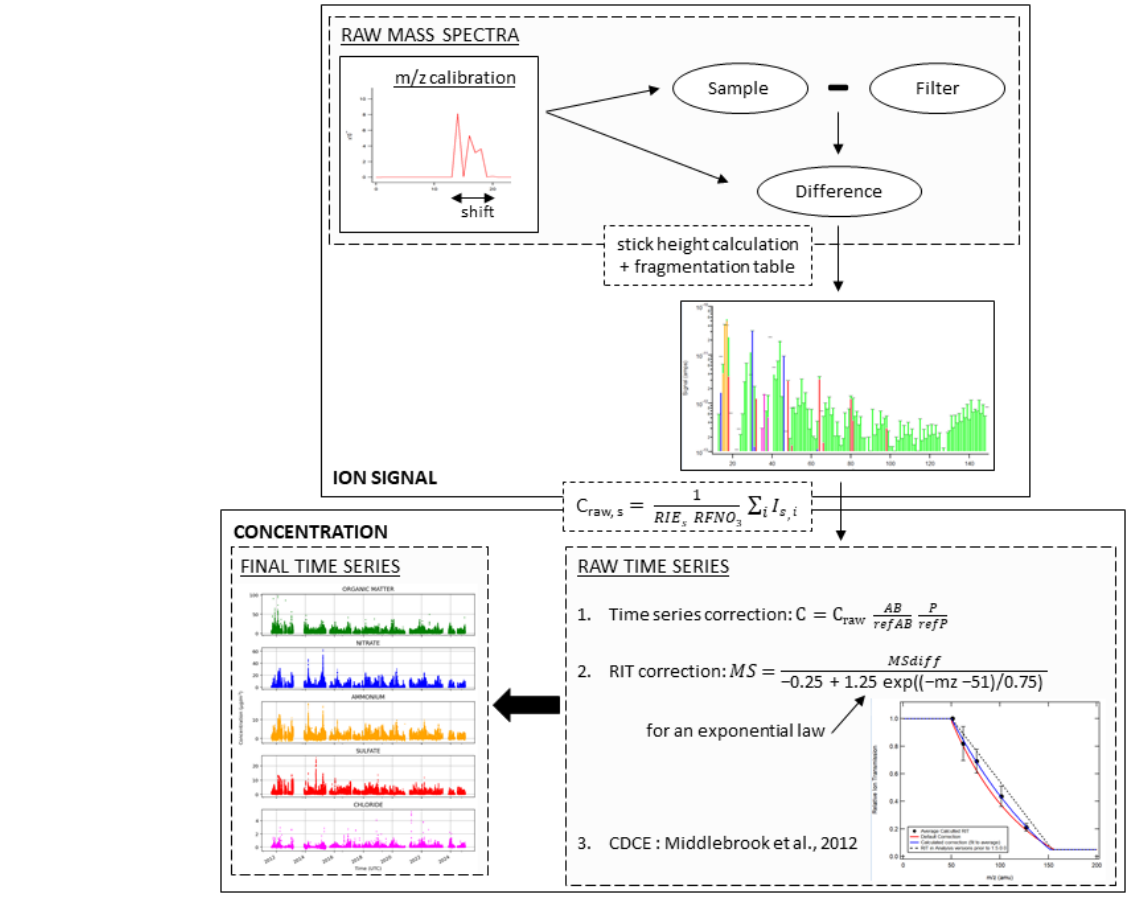

Figure 1. Steps of the process to the acquisition of concentration time series from the raw ion signal. $C_{raw,s}$ is the concentration of each species without any correction, based on the sum of the ion signal of their fragments $I_{s,i}$.

filter mode removes the particles, so that the difference provides the aerosol signal only. Equipped with a PM_1 lens, the particle beam is focused onto a standard vaporizer heated at 600°C. Vaporized particles are subsequently ionized by electronic impact at 70eV. Separation occurs for each fragment, having different mass-to-charge ratios (m/z), through a quadrupole mass analyzer (Ng et al., 2011). A diffusing source of Naphthalene inside the detection chamber provides an internal calibration standard and appears on both the mass spectra (MS) sample and filter, allowing m/z calibration and evaluation of the relative ion transmission efficiency (RIT) of the quadrupole, detailed below.

Prior to obtaining final concentrations, raw data are automatically processed through several steps summarized in Fig. 1. Briefly, the first step refers to an automatic m/z calibration of the open and closed signals, which consists of readjusting the center of each m/z based on the Naphthalene signal and other tracers (e.g., Ar, Kr, Ne, Xe, N_2O_2, $NaCO_2$, NOH, xxO_2). Then, the particle-only MS are subsequently calculated by subtracting the "closed" MS, measured in filter mode, from the "open" MS, measured in sample mode. The stick height of each peak gives its final ion signal, and thanks to a fragmentation table (Allan

https://doi.org/10.5194/essd-2026-490
Preprint. Discussion started: 11 August 2026

et al., 2004), each m/z is categorized into one of these species: organic matter (OM), nitrate, ammonium, sulfate, chloride. The response factor (RF) and relative ionization efficiency (RIE) values, determined by calibrating the instrument with known mass loadings of NH_4NO_3 and $(NH_4)_2SO_4$, are used to convert the ion signal into mass concentration. By default, the resulting MS are averaged over approximately 30 minutes, corresponding to 28 sets of sample-filter sequences.

Data are subject to several corrections through acquisition and post-processing. First, the "time series correction" compensates for variations in airbeam and pressure, normalized by the reference airbeam and pressure values (refAB and refP, respectively) obtained during the RF and RIE calibration. Secondly, signals of the different fragments of Naphthalene, normalized by the m/z 51 signal, in comparison with the theoretical signals from the NIST database, provide the relative ion transmission efficiency, which is usually described by an exponential or power law (Fig. 1). Therefore, the part of the MS between m/z 51 and 128 is weighted by the RIT fit, and the RIT for the rest of the MS is considered constant. Finally, the collection efficiency (CE) quantifies the particle losses occurring along their path from the aerodynamic lenses to their impact on the vaporizer, as defined in Ng et al. (2011). Indeed, their size and composition confer different properties to the particles (e.g., volatility, water content), influencing their trajectory and vaporization. The CE parameter is set to 0.5 by default for a standard vaporizer, and, following ACTRIS guidelines (WMO and GAW, 2016), adjusted point-by-point from the composition-dependent CE (CDCE) algorithm presented in Middlebrook et al. (2012). All those corrections are revised in post-processing to homogenize the long-term dataset.

2.3 Co-located ancillary measurements

2.3.1 Aethalometers

The Aethalometer (Magee Scientific) is a filter-based absorption photometer that enables the estimation of the aerosol absorption coefficients at seven different wavelengths (from 370nm to 950nm). From June 2011 to February 2013, an AE31 model was used, and the compensation was manually configured as presented in Petit et al. (2021). Since February 2013, measurements have been carried out using the newly developed AE33 model (Drinovec et al., 2015), providing data automatically compensated from the loading effect. Equivalent Black Carbon (eBC) concentrations were then derived following the ACTRIS recommendations and using a constant Mass Absorption Cross section (MAC) of 10.6m^2/g at 637nm, as detailed in Savadkoohi et al. (2024).

2.3.2 PM_1 mass concentration

From 2011 to 2016, PM_1 was determined using a Tapered Element Oscillating Microbalance (TEOM, 1400a model) equipped with a Filter Dynamic Measurement System (FDMS, 8500c model). The resulting TEOM-FDMS (Thermo Fisher Scientific) provided moving average concentrations (on hourly basis) every 15 min. From 2016 onwards, it has been replaced by a FIDAS (200 model, Palas) equipped with a polychromatic LED light source. The later instrument is an optical particle sizer deriving mass concentrations of PM_1, $PM_{2.5}$, PM_4 and PM_{10}. Both the TEOM-FDMS and the FIDAS have been demonstrated as

https://doi.org/10.5194/essd-2026-490
Preprint. Discussion started: 11 August 2026

Open Access Earth System Science Data Discussions

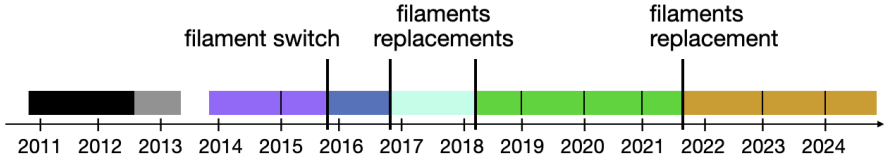

Figure 2. Time series of data processing procedures, each represented by a horizontal bar. Colors correspond to the different RF averages.

equivalent to the reference method defined by the European standardization committee (NF EN 16450; Amodeo (2023)) for (sub)urban background sites.

3 Homogeneous long-term data processing and validation

3.1 Data processing strategy

ACSM data processing has been optimized to analyze the dataset using the latest methods and knowledge, and to overcome the challenges posed by the operation of long-period measurements, such as the considerable amount of data and the discontinuities that can occur with multiple procedures. The strategy to homogenize the data stands in the revision of the processing parameters, listed in Appendix A1, to make them all consistent and to reduce their temporal variability caused by changes in protocol and instrument performance. Due to the large amount of raw data, the processing has been split into yearly files, ensuring consistency with the data submission requirements of ACTRIS. These different files are represented in Figure 2 where colors display different calibration factors, further detailed in Section 3.1.1. Data processing was performed on Igor 8 (Wavemetrics, Inc.) using acsm_local procedure v1.6.1.7, and the original fragmentation table developed by Allan et al. (2004). In order to evaluate any discrepancies caused by choices of processing from year to year, a 1-month common window was included. A preliminary screening of the data was conducted, utilizing notably airbeam variability and cross-referencing the different versions of the dataset, to identify periods when the instrument's behavior did not meet the required performance. This led to the discard of data from March to November 2013.

3.1.1 Response Factor and Relative Ionization Efficiencies

Obtained by calibration, RF and RIE values convert raw signals into interpretable ambient concentrations, thereby representing a critical aspect of data processing. They shall be specific to the filament and set-up in use, meaning that any replacement of filament and/or lens alignment maintenance can significantly modify RF and RIE values. We identified four filament changes since 2011. As RF/refAB and RIE values should be relatively stable between these breaking points, we considered calculating averages for these four different periods (Table 1). Additionally, a dedicated splitting was performed between 2011 and 2014, because of a different version of the acquisition software and tuning procedure. Indeed, until version v1.4.0.7, the SEM voltage tuning targeted a gain of 20,000 V instead of an airbeam of 1e-7 A, resulting in a variability of RF/refAB that needed to be

https://doi.org/10.5194/essd-2026-490
Preprint. Discussion started: 11 August 2026

Open Access Earth System Science Data Discussions

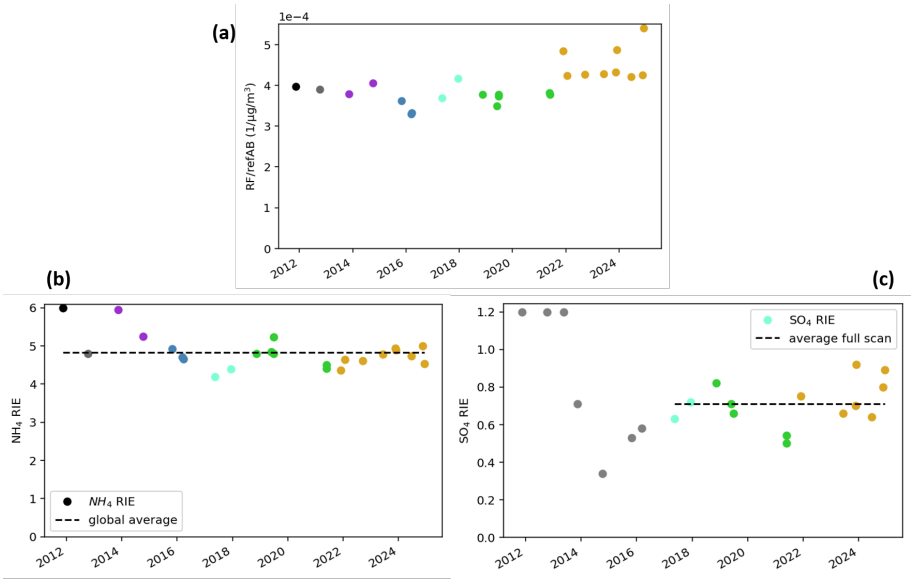

Figure 3. Time series of (a) RF/refAB ratios, (b) NH_4 RIE and (c) SO_4 RIE. Colors correspond to the RF averages and dotted lines to the RIEs averages.

taken into account. Finally, a critical inspection of recorded calibration data allowed to discard five calibration values, because of inconsistencies of calibration set-up or conditions. A total of 24 RF and RIE were used to calculate the different averages. Their temporal variability is presented in Figure 3.

Similar to the long-term processing of Poulain et al. (2020), no clear trend of RF/refAB or RIE is observed. Also, RF/refAB standard deviation varies between 5-10 % for each period, highlighting the fact that the intrinsic performance of the instrument can be stable over more than a decade. Since 2022, more frequent calibrations have been performed, revealing very satisfactory results. Because RIE should remain constant through time (Allan et al., 2004), single NH_4 and SO_4 RIE averages were calculated for the whole dataset. Since the NH_4 RIE is calibrated simultaneously with the NO_3 IE, its average is calculated according to the same calibrations selected for the NO_3 IE averages. The calibration was initially made in a "jump scan" mode, which consisted of measuring the signal of NH_4NO_3 and $(NH_4)_2SO_4$ main fragments only (m/z 30, 46 and 48, 64 respectively). In 2017, the calibration protocol changed to a "full scan" mode (FS), taking into account the entire mass spectrum as described in Freney et al. (2019). The scan mode of calibration has little impact on the response of NH_4NO_3, but since ammonium sulfate vaporizes at a slower rate, the FS calibration provides a more suitable SO_4 RIE, in addition to being more realistic compared to ambient measurements. Therefore, the average SO_4 RIE was calculated from the FS calibrations only (2017 onwards), and then extrapolated to the entire dataset. Average NH_4 and SO_4 RIEs used were 4.83 and 0.71, with a variability of 8.9 % and 16.9 %, respectively (Table 1).

In particular, the reprocessed SO_4 concentrations have been compared to SO_4 filter measurements conducted at the SIRTA observatory between June 2011 and June 2013. The concentrations of SO_4 using the averaged SO_4 RIE appear more consistent

https://doi.org/10.5194/essd-2026-490
Preprint. Discussion started: 11 August 2026

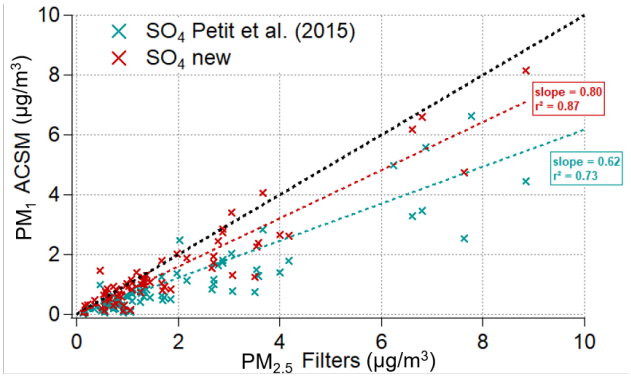

Figure 4. Comparison between ACSM SO_4 concentrations and SO_4 filter measurements. Data in blue are taken from Petit et al. (2015) and data in red are based on this study.

Table 1. Values of calibration parameters computed and used in the data reprocessing

RF/refAB (1/μg/m^3)	refAB (A)	Pref (mbar)	RIE NH_4	RIE SO_4
3.93e-04 ± 4.85e-06	5.94e-08 ± 1.96e-09	1.071 ± 0		
3.93e-04 ± 4.85e-06	7.48e-08 ± 4.10e-10	1.330 ± 0		
3.92e-04 ± 1.93e-05	1.02e-07 ± 3.11e-09	1.32 ± 0		
3.41e-04 ± 1.73e-05	9.84e-08 ± 1.53e-10	1.30 ± 3.61e-02	4.83 ± 0.43	0.71 ± 0.12
3.93e-04 ± 3.36e-05	9.37e-08 ± 5.30e-09	1.30 ± 2.19e-02		
3.73e-04 ± 1.17e-05	1.01e-07 ± 0	1.33 ± 3.40e-02		
4.52e-04 ± 4.21e-05	9.80e-08 ± 1.99e-09	1.29 ± 4.32e-02		

with SO_4 filter measurements (slope of 0.80) compared to the linear regression presented in Petit et al. (2015) (slope of 0.62; see Fig. 4). This result highlights the improved consistency between the ACSM dataset and external measurements, made possible by the reprocessing approach. Thus, specific attention will be dedicated to the analysis of SO_4 measurements in Section 4.3.

3.1.2 Ion transmission and mass calibration

One RIT and its fit were calculated for each year of data. Based on those calculations, three new fits were defined as three different RIT patterns were identified (Fig. 5). The first curve corresponds to the 2012 data and is applied only to the 2012 experiment due to its unique pattern. The second curve represents the average of the 2013 and 2014 RIT, and this fit is then applied to the 2013 and 2014 data, because both years presented a similar RIT behavior (within their standard deviation range). Finally, the last curve describes the RIT average from 2015 to 2024, as these data have a particularly comparable RIT pattern. This variation in the pattern may be related to the change in the tuning procedure implemented in 2014 and to detector sensitivity variability.

https://doi.org/10.5194/essd-2026-490
Preprint. Discussion started: 11 August 2026

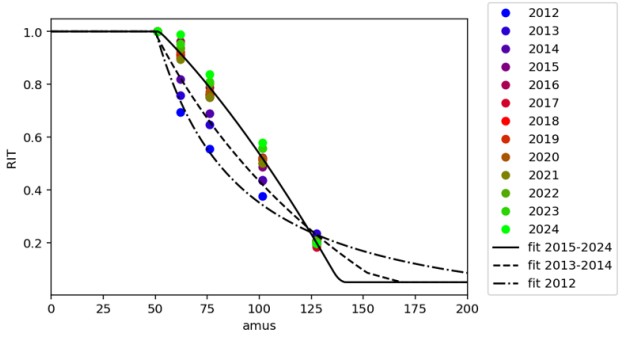

Figure 5. Annual RIT data and RIT fits over 3 different periods

A setting rarely questioned and that doesn't appear on the interface of the acsm_local, is the post-processing m/z calibration. It is applied by default in every data processing experiment while the data are loaded and consists of a shift in the MS so that the peaks are fitted correctly. This setting is meant to compensate for the lack of m/z calibration during the acquisition, thus it should not significantly affect the data if regular calibrations are done. At relatively low concentrations, the deactivation of this feature does not significantly impact the concentration values; however, the user should be aware of its existence and that it can lead to small variations in concentration. Indeed, small discrepancies were observed for the first overlap between 2014 and 2015 procedures, which were attributed solely to the variability in the RIT correction and m/z calibration. $NRPM_1$ concentrations show a very low sensitivity to this variability (slope = 1.007, r^2 = 1.0). Because differences were found only at the end of 2014, this suggests that the change of tuning, occurring at the same time and mentioned in Section 3.1.1, is the cause.

3.2 Validation and mass closure

After the application of new response factors and RIEs and the correction of RIT, two layers of validation processing were implemented to exclude unsatisfactory points. The first layer is an automatic process based on technical metrics, such as airbeam, inlet pressure, vaporizer temperature, limit of detection, concentrations, and number of sets during acquisition. The data were selected according to thresholds applied to these parameters values, corresponding to a standard operation of the ACSM and good quality measurements. The second layer is a manual flagging process consisting of identifying malfunctioning events and based on the recommendations of ACTRIS. This concerns the voltages of the heater bias and detector, and the emission current, as well as all unusual maintenance recorded throughout the operation of the instrument. During this validation process, approximately 16,000 points were discarded, resulting in the validation of 91 % of the data and a time coverage of 70 % between September 2011 and December 2024. This makes the SIRTA dataset (Petit, J.-E. and Brochet, J. and ACTRIS and GAW-WDCA, 2025) the first reprocessed and one of the longest time series worldwide, where robustness and quality have been ensured, while preserving a high data coverage (Fig. 6).

https://doi.org/10.5194/essd-2026-490
Preprint. Discussion started: 11 August 2026

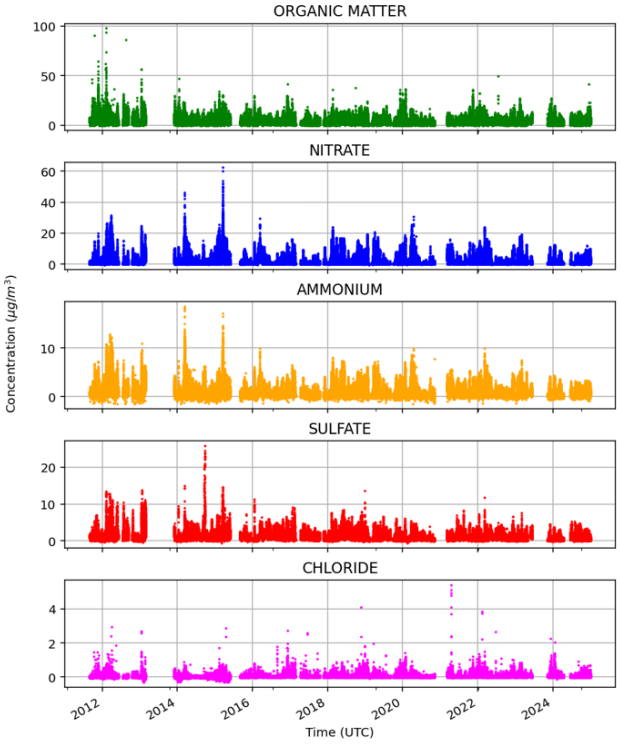

Figure 6. Mass concentrations of ACSM species from September 2011 to December 2024

To ensure the consistency of this dataset, a mass closure and an ion balance have been performed, after applying the composition-dependent collection efficiency (CDCE) determined in Middlebrook et al. (2012). First, the mass closure compares the PM_1 mass loading measured by the ACSM and Aethalometer with the TEOM-FDMS and FIDAS data, as described in 2.3. Figure 7 shows a good consistency between the PM_1 concentrations measured by the ACSM and Aethalometer and the total mass of PM_1 measured by the TEOM-FDMS or FIDAS, with a slope of 0.86 and a correlation coefficient of 0.82. The ion balance, which compares a theoretical concentration of NH_4 calculated from the concentrations of SO_4^{2-}, Cl^- and NO_3^+, and the measurements of NH_4, presents a slope close to 1 and a good correlation of 0.93 (Appendix A1).

3.3 Collection Efficiency evaluation

Introduced by Middlebrook et al. (2012) for standard vaporizers, CE may vary depending on sampling relative humidity (RH), aerosol acidity and composition. As a result, CE can be corrected following parameterizations to achieve a better capture of $NRPM_1$ mass concentrations. Little studies have re-evaluated the parameterization proposed in Middlebrook et al. (2012), and especially not for 10+-year datasets, which contain both business-as-usual and special event data. That is why we present here such an evaluation taking advantage of our validated ACSM dataset, along with the necessary collocated measurements of PM_1 and eBC, as described in Sect. 2.3. Fig. 8 presents the variation of the ratio between $NRPM_1$ measured by the ACSM with a

https://doi.org/10.5194/essd-2026-490
Preprint. Discussion started: 11 August 2026

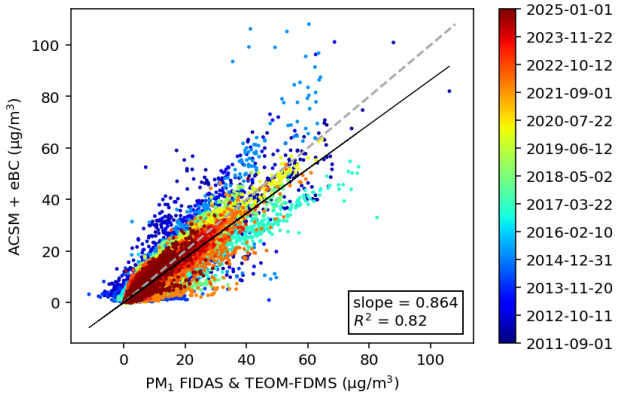

Figure 7. Mass closure of PM_1 (ACSM + eBC) compared to TEOM-FDMS and FIDAS measurements

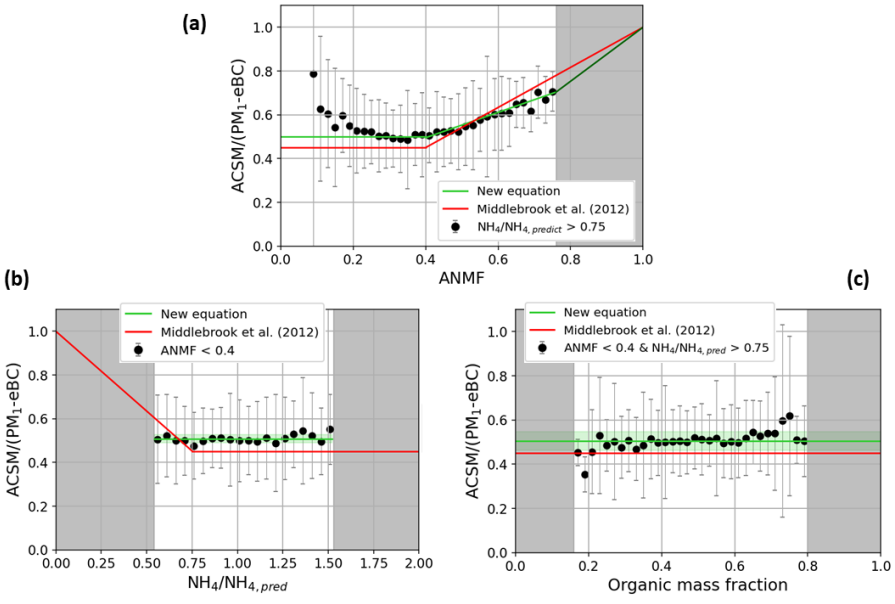

Figure 8. Mass closure of PM_1 ACSM measurements according to the (a) ANMF, (b) acidity and (c) organic content. The red line represents the Middlebrook et al. (2012) equation and the green line represents the new equation based on the SIRTA dataset with its standard deviation in light green. Error bars represent the interquartile range. Grey areas highlight the lack of extreme values in the dataset.

CE of 1 and (PM_1-eBC), depending on aerosol acidity, ammonium nitrate mass fraction (ANMF) and organic content. Red lines show the original parameterization from Middlebrook et al. (2012), while green lines show new equations obtained from our dataset.

In the case of low aerosol acidity ($NH_{4,meas}/NH_{4,pred} > 0.75$), variations appear following ANMF, especially when it gets higher than 0.4, and that ammonium is higher than the limit of detection. Our results suggest that, in this case, the minimum CE

https://doi.org/10.5194/essd-2026-490
Preprint. Discussion started: 11 August 2026

should be 0.5 instead of 0.45. It is interesting to note that the parametrization of Middlebrook et al. (2012) was calculated based on the bowing of the mass closure starting at ANMF = 0.4, and the theoretical CE of 1 in the case of pure ammonium nitrate particles (ANMF = 1). In our case, we observe that the original parameterization remains within the interquartile range of the $NRPM_1$/(PM_1-eBC) ratio, but with a change of slope from 0.9167 to 0.5701, occurring for ANMF = 0.5 instead of 0.4. In the second case, Middlebrook et al. (2012) demonstrated a linear relation between the ACSM concentrations and aerosol acidity when this acidity is high ($NH_{4,meas}/NH_{4,pred}$ < 0.75) and the ammonium nitrate content is low (ANMF < 0.4). However, no influence of the aerosol acidity was observed on the concentrations, thus the $NRPM_1$/(PM_1-eBC) ratio remains constant at 0.51 $\pm$ 0.014 (Fig. 8b). Finally, the same concentration behavior with respect to organic matter content was observed in Middlebrook et al. (2012) and in the new dataset, indicating no dependence between the two. While the constant in Middlebrook et al. (2012) is 0.45, the new dataset suggests a constant of 0.52 $\pm$ 0.034, which stays consistent with the results of the two previous cases. This new equation also raises questions about the behavior of CE in a gray zone (ANMF higher than 0.76; $NH_{4,meas}/NH_{4,pred}$ below 0.54 and above 1.53, organic content below 0.8 and above 0.16), where no data have ever been recorded. Even though the slope of our equation for ANMF > 0.4 is significantly different from that reported in Middlebrook et al. (2012), it is worth noting that its application to our reprocessed dataset does not lead to significant discrepancies (slope=1.001, r^2=0.997). Therefore, for the sake of consistency with previous datasets, it was decided to keep the original parameterization except for the minimum CE (0.5 has been used instead of 0.45). Nonetheless, this work highlights the interest of a more global evaluation of CE parameterizations, especially with the accumulation of long-term datasets in different kinds of environments. This would lead to a better assessment of the uncertainties associated with this correction.

4 Results and discussions

4.1 Long-term trend analysis

The extensive and unique temporal coverage of continuous ACSM measurements at SIRTA since Autumn 2011 enables the use of statistical tools to study the long-term variability of the major chemical composition of submicron aerosols. The Mann-Kendall method was applied, using the pyMannKendall Python package developed by Hussain and Mahmud (2019). The Mann-Kendall method is a non-parametric test for identifying trends in time series containing no serial correlation or seasonal effects (Collaud Coen et al., 2020). As this test was applied to annual averages, no seasonal patterns were observed and its autocorrelation stayed below 50 %. Only trends at the 95 % confidence level (p<0.05) are considered statistically significant. Figure 9 presents the results of the trend analysis, both on global and seasonal aspects, and all values are detailed in Table A2.

Globally, PM_1 concentrations are decreasing at an average rate of 0.34 $\mu g/m^3$ per year at SIRTA. Looking into the composition of $NRPM_1$, NH_4 and SO_4 are the only components presenting a significant diminishing trend of 0.05 $\mu g/m^3$ and 0.044 $\mu g/m^3$ per year, respectively (Fig. 9). Since ammonium sulfate is mainly advected onto the Paris region (e.g. Petit et al. (2015)), this illustrates the decrease of SO_2 emissions in Europe (European Topic Centre on Air pollution, transport, noise and industrial pollution et al., 2020). This result is also supported by the significant reduction in total PM_1 mass concentration in Eastern air masses reported in Atabakhsh et al. (2025), as the majority of SO_4 mass concentration in the Paris region comes

https://doi.org/10.5194/essd-2026-490
Preprint. Discussion started: 11 August 2026

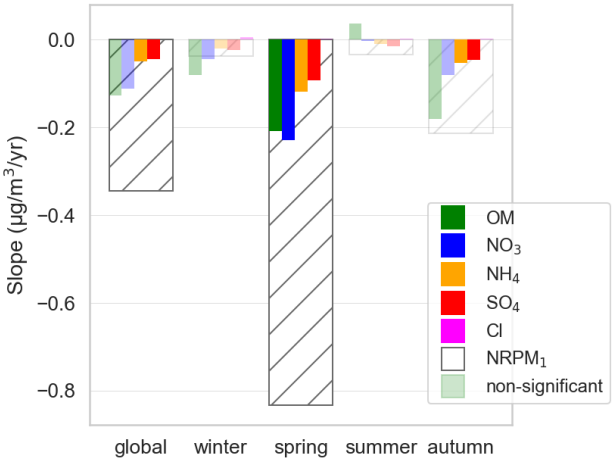

Figure 9. Global and seasonal trend slopes of NR-PM_1 components. Significant trend slopes are represented in bright colors, others are non-significant.

from the Eastern European industrial sector (Schneider et al., 2025). This dataset could also benefit from a separate analysis of western and eastern air masses to identify the cause of aerosol reduction. A decreasing PM_1 trend has also been observed at the Melpitz background station in Germany (Atabakhsh et al., 2025). This shows the interest in multiple trend analysis in Europe in order to map the aerosol variability. Comparing long-term datasets in numerous sites will help better describe the effects of meteorological conditions, long-range transport and atmospheric circulation processes in general.

However, these results differ from previous trend analysis carried out at SIRTA (Zhang et al. (2019); Petit et al. (2021)), which are summarized in Table 2. There are first discrepancies in compounds exhibiting a significant decreasing trend, especially SO_4 and NH_4. This feature may certainly be resulting from the reprocessing procedure, since these are the two compounds most prone to change, due to the revision of their RIEs. The original dataset, studied in previous publications, used SO_4 RIE of 1.2, or jump scan value, before 2017, whereas a homogeneous RIE of 0.71 is now implemented, leading to increased concentrations during 2012-2017 and, therefore, favoring a more significant decreasing trend. As a result, we highlight here the relevance of ACSM data reprocessing for long-term trends, especially for measurements conducted before 2017. For the other compounds (OA and NO_3), differences may also come from the extended temporal coverage, as well as, for OA, compensatory variations of OA fractions. It could also be argued that 6 or 8 years of measurements may not be sufficient to robustly capture long-term variations. Nevertheless, our results are in good agreement with previous studies suggesting overall decreasing trends for the PM chemical compounds in Europe over the past decades (e.g., Tørseth et al. (2012); Pandolfi et al. (2016); Tsyro et al. (2022); Tsimpidi et al. (2025)).

At the seasonal scale, spring demonstrates the highest variability of $NRPM_1$ components with decreasing concentrations of OM, NO_3, NH_4 and SO_4 (-0.21, -0.23, -0.12 and -0.09 $\mu g/m^3/yr$, respectively). Spring is also the most polluted season, with the highest particle loadings in the Paris region (Petit et al. (2015); Bressi et al. (2021)) and frequent persistent pollution

https://doi.org/10.5194/essd-2026-490
Preprint. Discussion started: 11 August 2026

Open Access Earth System Science Data Discussions

Table 2. Sen's slope in $\mu g/m^3/yr$ from Mann-Kendall trend analysis from different studies at SIRTA. Only slopes associated to p<0.05 are displayed, non-statistically representative (nsr) is noted otherwise. Grey cells correspond to compounds not investigated.

	This study	**Zhang et al. (2019)**	**Petit et al. (2021)**	**Bouillon et al. (2025)**
OM	nsr	-0.3823	-0.068	
NO_3	nsr	nsr	-0.037	
SO_4	-0.05	nsr	nsr	
NH_4	-0.044		nsr	
Cl	nsr		nsr	
eBC_{sf}		nsr	nsr	nsr
eBC_{lf}		-0.004	-0.018	-0.024
PM_1	-0.34 ($NRPM_1$)	nsr	nsr	

episodes dominated mainly by secondary compounds (NO_3 and secondary OA). As shown in Zhang et al. (2019), among the components of OA, the more-oxidized fraction (MO-OOA) has the main contribution in Spring and is the one exhibiting the steepest decrease (also found in Petit et al. (2021)). Therefore, beyond the discrepancies shown in Table 2, it is likely that the OA decrease between 2012 and 2024 during Spring is strongly related to secondary OA. Zhang et al. (2019) suggested that the reduction in MO-OOA was partially caused by the reduction in anthropogenic volatile organic compounds (VOCs) emissions in France and western Europe during 2012-2017. Long-term source apportionment could provide further details on the composition of primary and secondary OA components and their temporal variability over more than 10 years. The decrease of springtime $(NH_4)_2SO_4$ is still related to a reduction of SO_2 industrial emissions in Eastern Europe, but also to a variation in the frequency of continental air masses, usually more frequent at this time of the year (see Appendix A2). As proposed in Meng et al. (2025), this dataset can act as an excellent case study to disentangle emission-related variations with meteorology-related ones. Finally, the sharp decrease of springtime NO_3 (-0.23$\mu g/m^3/yr$) can naturally be related to the observed decrease of NOx concentrations in the Paris region (-0.17ppb/yr for NO_2, Bouillon et al. (2025)), also supported by the observed decrease of eBC_lf concentrations. During the first COVID-19 lockdown in France (17/03/2020-11/05/2020), NO_3 was also found to decrease by 1.03$\mu g/m^3$, which corresponds to around 4.5 years of gradual decrease. Ammonium nitrate being also one of the dominant components of pollution episodes, this dataset can be a valuable asset to examine the variability of persistent pollution episodes, which is described below.

4.2 Persistent pollution episodes

Persistent pollution episodes (PPE) refer to periods when the daily PM_1 concentration exceeds 20 $\mu g/m^3$ for at least 3 consecutive days (Petit et al., 2015). The development of long-term datasets enables the study of PPE variability. Figure 10 presents the occurrence, duration and maximum concentration of PPE at SIRTA throughout the 13 years of measurements. First, a statistically significant decrease in the PPE occurrence has been observed between 2012 and 2024 of 5 % per year, from an average of 2.67 episodes per year between 2012 and 2017 to 0.5 per year in the most recent years (2021-2024) (Fig. 10). PPE

https://doi.org/10.5194/essd-2026-490
Preprint. Discussion started: 11 August 2026

lasted longer and reached higher concentrations between 2012 and 2015 than after 2016 (5 days and 41 μg/m^3 on average, against 3 days and 34 μg/m^3). Figure A3 might suggest a correlation between the maximum concentration and the duration of PPE, even though the scarcity of data for long and highly concentrated PPE prevents the use of statistical tools. This relation can be partly linked to stable meteorological conditions (low temperature, wind speed, and mixing layer height), as they can favor the accumulation of aerosols in the troposphere (Pope et al. (2015); Stirnberg et al. (2021)). Moreover, the two most intense episodes occurred in the earliest period and were documented separately in Winter 2012 in (Petit et al., 2015) and in Spring 2015 (Petit et al., 2017a). The majority of the PPE occurred in Winter (50 %) and was driven by a strong contribution of OM (46 % on average), while around a third occurred in Spring (36 %) and was driven by a stronger fraction of secondary inorganic aerosol (67 %). Although OA source apportionment shall provide precise information, previous studies at SIRTA have highlighted that the winter fraction of OM can be related to residential wood burning (Zhang et al., 2019) and can be enhanced by low temperatures, leading to higher local emissions and important particle formation processes (Stirnberg et al., 2021). As exposed in Petit et al. (2017a), climatological parameters, such as sea-level pressure anomalies and rainfall shortage, can modulate PPE, which are related to large-scale meteorological systems. As a result, analyzing synoptic weather regimes at a larger scale could provide more detail on PPE formation (Jones and Lister, 2009). Typical meteorological conditions can be grouped into four higher-scale circulation patterns, called weather regimes, distinguished into two "cyclonic" regimes, positive and negative North Atlantic Oscillation (NAO+ and NAO-), and two "anticyclonic" regimes, Atlantic Ridge (AR) and Blocking (BL) (Ferranti et al. (2015); Grams (2026)). By attributing weather regimes to the PPE in the Paris region, 59 % of them occurred under blocking conditions (54.5 % BL and 4.5 % AR), suggesting again that adverse synoptic conditions can encourage the accumulation of PM_1 within the troposphere. The reported increase in the frequency of anticyclonic regimes (Ferranti et al. (2015); Grams (2026)) suggests a higher occurrence and intensity of PPE as well. However, the decrease of PPE occurrence and intensity at SIRTA suggests that the reduction of emissions compensates for the increasing frequency of blocking weather regimes and that the effects of mitigation might be minimized by these changes in atmospheric circulations.

More globally, the temporal coverage of our dataset at SIRTA enables climatological-based analysis, which should be further examined regarding individual components such as SO_4 following long-range transport patterns, and OA subfractions for additional information on the contributions of primary and secondary sources during PPE.

4.3 Trajectory analysis reveals S-containing particles source apportionment

Concentration-weighed Trajectory (CWT) has been performed coupling SO_4 concentrations with air mass backtrajectories between 2011 and 2024. 120-h backtrajectories were calculated each hour from HYSPLIT (Stein et al., 2015) and GDAS input files at a 1°x1° spatial resolution. Backtrajectories and CWT calculations were supervised by ZeFir (Petit et al., 2017b). The overall analysis (Fig. 11) largely confirms the main contribution of continental advection of SO_4, originating from SO_2 emissions within Eastern Europe. This feature was notably highlighted during a recent multi-site trajectory analysis across Europe (Schneider et al., 2025). Interestingly, annual analyses don't show significant variability in the geographical contributions from Eastern Europe. They, however, spotlight sporadic contributions from Iceland, notably in 2014 (Boichu et al., 2019), 2020, and to a lesser extent in 2023 and 2024 (11). These generally come from short-term events lasting no more than a few days. As

https://doi.org/10.5194/essd-2026-490
Preprint. Discussion started: 11 August 2026

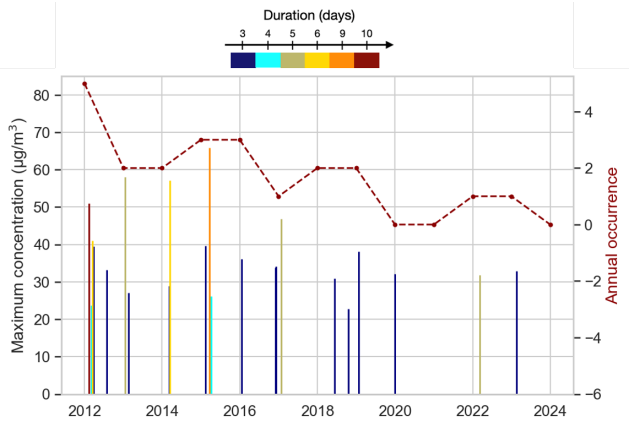

Figure 10. Maximum concentration in $\mu g/m^3$ (vertical lines) and annual occurrence (red dashed line) of PPE since 2012. The colors of the vertical lines indicate the duration of each event in days.

such, they can be rather easily spotted from a timeseries. Nevertheless, volcanic and anthropogenic SO_4 fragment the same way, making it hard to apportion from aerosol mass spectrometer data when they co-occur, and without more advanced statistical analysis. Also, as reported by Carn et al. (2017), volcanic SO_2 emissions are driven by passive degassing rather than eruptive plumes. Beyond noticeable events associated with major eruptions, our results underline the need for proper attribution.

Additionally, although previous measurements in the Paris region have highlighted contributions of marine organic aerosols (MOA), either on filter-based (Bressi et al., 2013) or aerosol mass spectrometer (Crippa et al., 2014) measurements, this fraction has never been identified from ACSM measurements at SIRTA. This may originate from the lower sensitivity of ACSM compared to low concentration compounds such as methylsulfonic acid (MSA). Unit-mass resolution may also limit the unambiguous identification of corresponding ion like $CH_3SO_2^+$ (m/z 79). However, long-term variability of f_{79} at SIRTA reveals a seasonality consistent with the one expected by phytoplanktonic activities in the North Atlantic Ocean and Northern Seas (Fig. 12a), as well as MSA. Trajectory analysis of f_{79} between 2011 and 2024 confirms a clear oceanic origin (Fig. 12b). Therefore, despite rather low concentrations, future source apportionment studies of OA at SIRTA shall include MOA constraints. This may also be the case at other sites within North-Western Europe. More generally, it highlights the need for further source apportionment of S-containing particles (both inorganic and organic), as well as proper meteorological guidelines in terms of RIE.

5 Conclusions and recommendations

At the SIRTA observatory, PM_1 composition has been continuously monitored for over 13 years using a Q-ACSM and an Aethalometer, while co-located instrumentation measured the total mass of PM_1, constituting one of the longest time series worldwide. The emergence of long-term datasets has raised both new interests and challenges for characterizing aerosol variability. However, discontinuities might be observed within the dataset due to the evolution of knowledge, the progressive

https://doi.org/10.5194/essd-2026-490
Preprint. Discussion started: 11 August 2026

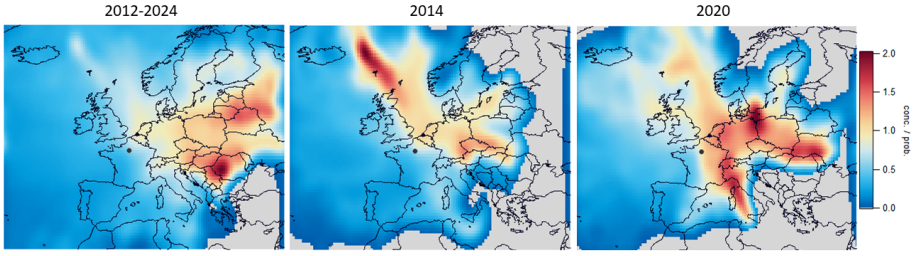

Figure 11. Global, 2014 and 2020 backtrajectories of SO_4 concentrations over Europe

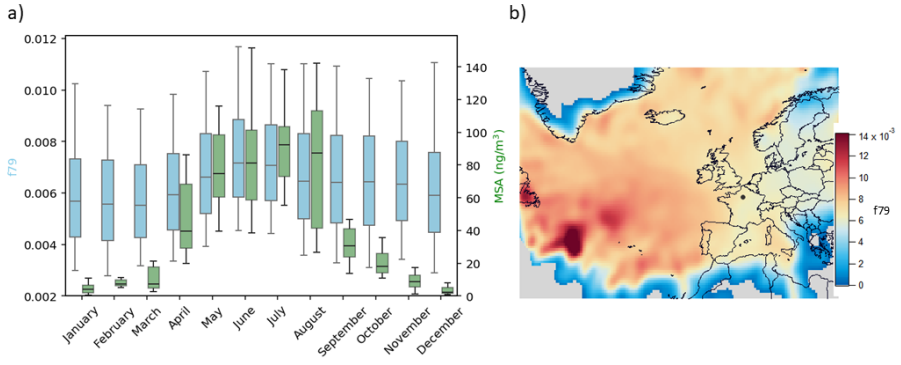

Figure 12. (a) Monthly concentrations of 2011-2024 ACSM f_{79} (blue) and 2009-2010 filter-based Methylsulfonic acid (MSA, green). (b) Backtrajectories of f_{79} over the 2011-2024 period.

development of standard operating procedures, and the succession of different operators. Therefore, this study aims to reduce the variability and uncertainties linked to these factors.

To answer these questions, a new approach to data reprocessing has been developed. This involved revising calibration parameters and corrections to optimize the existing measurements and instrument operation. Due to their direct involvement in concentration calculations, refining RF and RIE values has been identified as a key factor in reprocessing. Corrections, in terms of ion transmission and mass calibration, were also revised, demonstrating a low sensitivity in the concentrations. This dataset presents a valuable resource, thanks to its size and robustness, for evaluating the CDCE parameterization and utilizing the Mann-Kendall method for trend analysis. Results of the CDCE evaluation show small discrepancies between Middlebrook et al. (2012) equation and the new one, and even smaller impacts on NR-PM_1 concentrations; even though this dataset lacks extreme values in terms of acidity, ammonium nitrate and organic content. In this sense, this study could benefit from other long-term datasets that present different features.

On the other hand, interesting applications for long-term datasets have been presented, involving the characterization of PM_1 variability, persistent pollution episodes, and Sulfate source apportionment. PM_1 have decreased by 0.34 $\mu g/m^3$/yr between 2012 and 2024, in contrast with the absence of a significant trend within the original dataset, which highlights the impact and, subsequently, the importance of reprocessing for data interpretation. NH_4 and SO_4 demonstrate similar variability at the annual

https://doi.org/10.5194/essd-2026-490
Preprint. Discussion started: 11 August 2026

scale and in Autumn. Spring, with maximum concentrations, presents significant decreasing trends for the majority of the NR-PM_1 components, ranging from -0.093 $\mu g/m^3$/yr for SO_4 to -0.23 $\mu g/m^3$/yr for NO_3. The contribution of both local sources and long-range transport makes the impacts of national and European mitigation difficult to identify. Nevertheless, these results indicate an encouraging trend in atmospheric aerosol pollution. Similarly, the evolution of PPE shows a decreasing trend in their occurrence by 5 % since 2012. Half of these episodes occurred in Winter, where OM contributed to 46 % of mass concentration and 36 % were observed in Spring, driven mostly by secondary inorganic aerosol concentrations (67 %). The maximum concentration and the duration of PPE seem correlated and appear to be linked to stable meteorological conditions (Petit et al., 2017a) and, to a greater extent, to blocking weather regimes (Ferranti et al. (2015) ; Grams (2026)), as 59 % of PPE occurred under blocking conditions.

Overall, the approach of data reprocessing has proven essential in the interpretation of long-term time series and their special features. In hindsight, the traceability of repairs and the operation protocol of the instrument should be treated with special care, as well as multiplying RF and RIEs calibrations to better understand the data. Finally, the homogenization of long-term datasets could become a valuable aspect within the ACTRIS framework, in order to develop standard data processing protocols and facilitate the comparison of measurements between different stations.

Data availability. The reprocessed ACSM dataset at SIRTA is available in EBAS database at https://doi.org/10.48597/4RKH-6RDU (Petit, J.-E. and Brochet, J. and ACTRIS and GAW-WDCA, 2025). AE33 data are available in the Easy Data catalog at https://doi.org/10.57932/5c399263-a317-41b7-8900-184b177c4216 (Ramonet, M. and Bouillon, L., 2025).

Appendix A

Table A1. Parameters revised for the reprocessing, in order of priority according to the concentration sensitivity

Response factor (RF)
Relative ionization efficiencies (RIEs)
Time series correction (pressure, airbeam)
Relative ion transmission (RIT)
Mass calibration (m/z cal)

https://doi.org/10.5194/essd-2026-490
Preprint. Discussion started: 11 August 2026

Open Access Earth System Science Data Discussions

Table A2. Trend slopes (p-value) of ACSM species over the whole period and in each season. Significant trends are in bold text.

slope (p-value)	**Global**	**Winter**	**Spring**	**Summer**	**Autumn**
OM	-0.13 (0.077)	-0.081 (0.13)	**-0.21 (0.012)**	0.036 (0.88)	-0.18 (0.10)
NO_3	-0.11 (0.13)	-0.44 (0.50)	**-0.23 (0.0060)**	-0.0038 (0.88)	-0.081 (0.10)
NH_4	**-0.050 (0.044)**	-0.020 (0.43)	**-0.12 (0.0041)**	-0.0096 (0.88)	**-0.053 (0.024)**
SO_4	**-0.44 (0.0041)**	-0.023 (0.43)	**-0.093 (0.00032)**	-0.015 (0.35)	**-0.046 (0.044)**
Cl	0.0011 (0.25)	0.0050 (0.20)	0.0020 (0.43)	0.0018 (0.21)	0.0016 (0.58)
$NRPM_1$	**-0.34 (0.024)**	-0.037 (0.76)	**-0.83 (0.012)**	-0.034 (1.0)	-0.21 (0.15)

https://doi.org/10.5194/essd-2026-490
Preprint. Discussion started: 11 August 2026

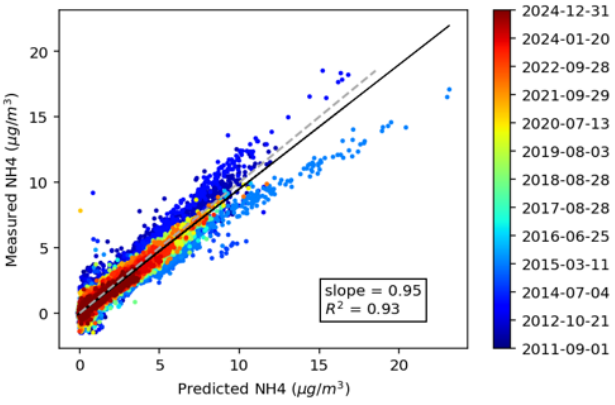

Figure A1. Ion balance of ACSM measurements between September 2011 and December 2024

https://doi.org/10.5194/essd-2026-490
Preprint. Discussion started: 11 August 2026

Open Access Earth System Science Data Discussions

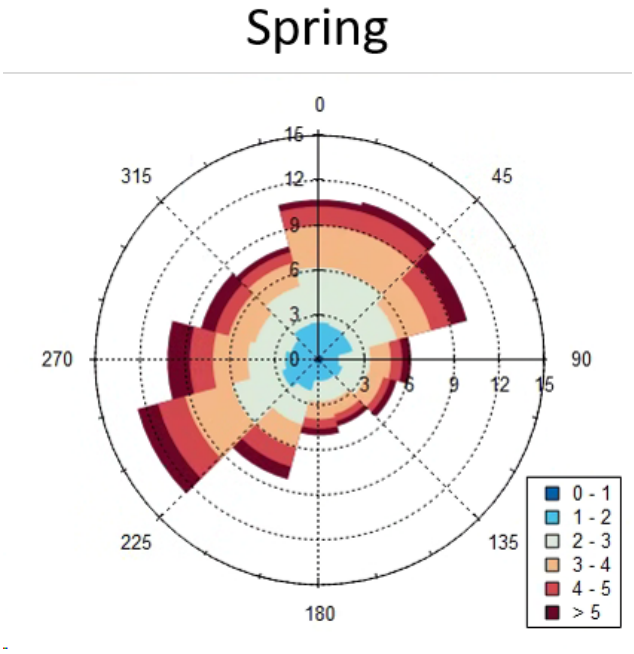

Figure A2. Direction of wind in Spring at the SIRTA observatory. The radial axis indicates the frequency, and the colors represent the wind speed in m/s.

https://doi.org/10.5194/essd-2026-490
Preprint. Discussion started: 11 August 2026

Open Access Earth System Science Data Discussions

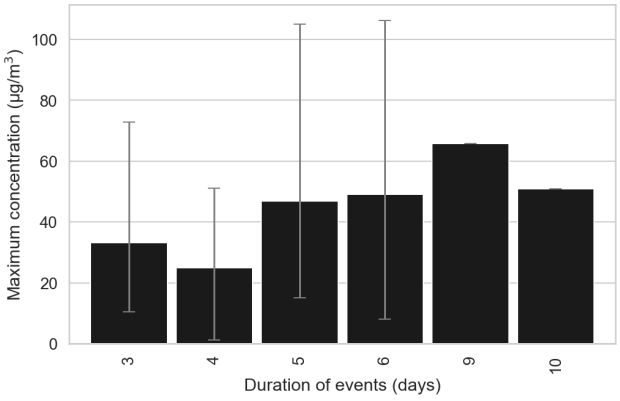

Figure A3. Median of maximum concentration regarding the duration of PPE. The grey bars represent the range between the lowest and highest values of maximum concentrations.

Author contributions. J.B. and J-E.P. developed the methodology and carried out the investigation and visualization. J.B. and L.C. conducted the formal analysis. A.B. J-E.P., T.A., Y.Z., V.C., P.C., J.B., H.C. and O.F. managed the data curation. J.B. and J-E.P. prepared the original draft and all co-authors participated in the review and editing process. J-E.P., V.G. and O.F. provided the supervision.

Competing interests. The authors declare that they have no conflict of interest.

Acknowledgements. The authors gratefully acknowledge CNRS-INSU for supporting measurements performed at the SI-SIRTA, and those within the long-term monitoring aerosol program SNO-CLAP, both of which are components of the ACTRIS French Research Infrastructure. This work was also supported by CEA. The authors also thank Jean Sciare, François Truong, Caroline Marchand, and technicians, engineers and scientists from INERIS for their contributions to implementing or monitoring aerosol in situ measurements at SIRTA. Data used in this study were accessed from EBAS (https://ebas.nilu.no) hosted by NILU. Specifically, the use included data affiliated with the framework: ACTRIS-EU, GAW-WDCA.

https://doi.org/10.5194/essd-2026-490
Preprint. Discussion started: 11 August 2026

References

Allan, J. D., Delia, A. E., Coe, H., Bower, K. N., Alfarra, M., Jimenez, J. L., Middlebrook, A. M., Drewnick, F., Onasch, T. B., Canagaratna, M. R., Jayne, J. T., and Worsnop, D. R.: A generalised method for the extraction of chemically resolved mass spectra from Aerodyne aerosol mass spectrometer data, Journal of Aerosol Science, 35, 909–922, https://doi.org/10.1016/j.jaerosci.2004.02.007, 2004.

Amodeo, T.: Guide méthodologique pour la surveillance des PM10 et PM2,5 dans l'air ambiant par FIDAS, Tech. rep., LCSQA, INERIS, https://www.lcsqa.org/fr/rapport/guide-methodologique-pour-la-surveillance-des-pm10-et-pm25-dans-lair-ambiant-par-methode-0, 2023.

Atabakhsh, S., Poulain, L., Bigi, A., Coen, M. C., Pöhlker, M., and Herrmann, H.: Trends of PM1 aerosol chemical composition, carbonaceous aerosol, and source over the last ten years at Melpitz (Germany), Atmospheric Environment, p. 121075, https://doi.org/10.1016/j.atmosenv.2025.121075, 2025.

Beelen, R., Raaschou-Nielsen, O., Stafoggia, M., Andersen, Z. J., Weinmayr, G., Hoffmann, B., Wolf, K., Samoli, E., Fischer, P., Nieuwenhuijsen, M., Vineis, P., Xun, W. W., Katsouyanni, K., Dimakopoulou, K., Oudin, A., Forsberg, B., Modig, L., Havulinna, A. S., Lanki, T., Turunen, A., Oftedal, B., Nystad, W., Nafstad, P., De Faire, U., Pedersen, N. L., Östenson, C.-G., Fratiglioni, L., Penell, J., Korek, M., Pershagen, G., Eriksen, K. T., Overvad, K., Ellermann, T., Eeftens, M., Peeters, P. H., Meliefste, K., Wang, M., Bueno-de Mesquita, B., Sugiri, D., Krämer, U., Heinrich, J., De Hoogh, K., Key, T., Peters, A., Hampel, R., Concin, H., Nagel, G., Ineichen, A., Schaffner, E., Probst-Hensch, N., Künzli, N., Schindler, C., Schikowski, T., Adam, M., Phuleria, H., Vilier, A., Clavel-Chapelon, F., Declercq, C., Grioni, S., Krogh, V., Tsai, M.-Y., Ricceri, F., Sacerdote, C., Galassi, C., Migliore, E., Ranzi, A., Cesaroni, G., Badaloni, C., Forastiere, F., Tamayo, I., Amiano, P., Dorronsoro, M., Katsoulis, M., Trichopoulou, A., Brunekreef, B., and Hoek, G.: Effects of long-term exposure to air pollution on natural-cause mortality: an analysis of 22 European cohorts within the multicentre ESCAPE project, The Lancet, 383, 785–795, https://doi.org/10.1016/S0140-6736(13)62158-3, 2014.

Boichu, M., Favez, O., Riffault, V., Petit, J.-E., Zhang, Y., Brogniez, C., Sciare, J., Chiapello, I., Clarisse, L., Zhang, S., Pujol-Söhne, N., Tison, E., Delbarre, H., and Goloub, P.: Large-scale particulate air pollution and chemical fingerprint of volcanic sulfate aerosols from the 2014–2015 Holuhraun flood lava eruption of Bárðarbunga volcano (Iceland), Atmospheric Chemistry and Physics, 19, 14 253–14 287, https://doi.org/10.5194/acp-19-14253-2019, 2019.

Bouillon, L., Gros, V., Lopez, M., Bonnaire, N., Philippon, C., Yver Kwok, C., David, L., Perrussel, O., Sanchez, O., Kotthaus, S., Petit, J.-E., Ciais, P., and Ramonet, M.: Ten years of measurements (2012–2022) of the atmospheric composition at Saclay/SIRTA Observatory in the Ile de France Region as part of ICOS and ACTRIS, https://doi.org/10.5194/essd-2025-602, ESSD [preprint], 2025.

Bressi, M., Sciare, J., Ghersi, V., Bonnaire, N., Nicolas, J. B., Petit, J.-E., Moukhtar, S., Rosso, A., Mihalopoulos, N., and Féron, A.: A one-year comprehensive chemical characterisation of fine aerosol (PM_{2.5}) at urban, suburban and rural background sites in the region of Paris (France), Atmospheric Chemistry and Physics, 13, 7825–7844, https://doi.org/10.5194/acp-13-7825-2013, 2013.

Bressi, M., Cavalli, F., Putaud, J., Fröhlich, R., Petit, J.-E., Aas, W., Äijälä, M., Alastuey, A., Allan, J., Aurela, M., Berico, M., Bougiatioti, A., Bukowiecki, N., Canonaco, F., Crenn, V., Dusanter, S., Ehn, M., Elsasser, M., Flentje, H., Graf, P., Green, D., Heikkinen, L., Hermann, H., Holzinger, R., Hueglin, C., Keernik, H., Kiendler-Scharr, A., Kubelová, L., Lunder, C., Maasikmets, M., Makeš, O., Malaguti, A., Mihalopoulos, N., Nicolas, J., O'Dowd, C., Ovadnevaite, J., Petralia, E., Poulain, L., Priestman, M., Riffault, V., Ripoll, A., Schlag, P., Schwarz, J., Sciare, J., Slowik, J., Sosedova, Y., Stavroulas, I., Teinemaa, E., Via, M., Vodička, P., Williams, P., Wiedensohler, A., Young, D., Zhang, S., Favez, O., Minguillón, M., and Prevot, A.: A European aerosol phenomenology - 7: High-

https://doi.org/10.5194/essd-2026-490
Preprint. Discussion started: 11 August 2026

time resolution chemical characteristics of submicron particulate matter across Europe, Atmospheric Environment: X, 10, 100 108, https://doi.org/10.1016/j.aeaoa.2021.100108, 2021.

Carn, S. A., Fioletov, V. E., McLinden, C. A., Li, C., and Krotkov, N. A.: A decade of global volcanic SO2 emissions measured from space, Scientific Reports, 7, 44 095, https://doi.org/10.1038/srep44095, 2017.

Chen, G., Canonaco, F., Tobler, A., Aas, W., Alastuey, A., Allan, J., Atabakhsh, S., Aurela, M., Baltensperger, U., Bougiatioti, A., De Brito, J. F., Ceburnis, D., Chazeau, B., Chebaicheb, H., Daellenbach, K. R., Ehn, M., El Haddad, I., Eleftheriadis, K., Favez, O., Flentje, H., Font, A., Fossum, K., Freney, E., Gini, M., Green, D. C., Heikkinen, L., Herrmann, H., Kalogridis, A.-C., Keernik, H., Lhotka, R., Lin, C., Lunder, C., Maasikmets, M., Manousakas, M. I., Marchand, N., Marin, C., Marmureanu, L., Mihalopoulos, N., Močnik, G., Nęcki, J., O'Dowd, C., Ovadnevaite, J., Peter, T., Petit, J.-E., Pikridas, M., Matthew Platt, S., Pokorná, P., Poulain, L., Priestman, M., Riffault, V., Rinaldi, M., Różański, K., Schwarz, J., Sciare, J., Simon, L., Skiba, A., Slowik, J. G., Sosedova, Y., Stavroulas, I., Styszko, K., Teinemaa, E., Timonen, H., Tremper, A., Vasilescu, J., Via, M., Vodička, P., Wiedensohler, A., Zografou, O., Cruz Minguillón, M., and Prévôt, A. S.: European aerosol phenomenology - 8: Harmonised source apportionment of organic aerosol using 22 Year-long ACSM/AMS datasets, Environment International, 166, 107 325, https://doi.org/10.1016/j.envint.2022.107325, 2022.

Chen, G. I., Tremper, A. H., Priestman, M., Font, A., and Green, D. C.: How COVID-19 related policies reshaped organic aerosol source contributions in Central London, Atmospheric Chemistry and Physics, 25, 14 825–14 838, https://doi.org/10.5194/acp-25-14825-2025, 2025.

Collaud Coen, M., Andrews, E., Bigi, A., Martucci, G., Romanens, G., Vogt, F. P. A., and Vuilleumier, L.: Effects of the prewhitening method, the time granularity, and the time segmentation on the Mann–Kendall trend detection and the associated Sen's slope, Atmospheric Measurement Techniques, 13, 6945–6964, https://doi.org/10.5194/amt-13-6945-2020, 2020.

Crippa, M., Canonaco, F., Lanz, V. A., Äijälä, M., Allan, J. D., Carbone, S., Capes, G., Ceburnis, D., Dall'Osto, M., Day, D. A., DeCarlo, P. F., Ehn, M., Eriksson, A., Freney, E., Hildebrandt Ruiz, L., Hillamo, R., Jimenez, J. L., Junninen, H., Kiendler-Scharr, A., Kortelainen, A.-M., Kulmala, M., Laaksonen, A., Mensah, A. A., Mohr, C., Nemitz, E., O'Dowd, C., Ovadnevaite, J., Pandis, S. N., Petäjä, T., Poulain, L., Saarikoski, S., Sellegri, K., Swietlicki, E., Tiitta, P., Worsnop, D. R., Baltensperger, U., and Prévôt, A. S. H.: Organic aerosol components derived from 25 AMS data sets across Europe using a consistent ME-2 based source apportionment approach, Atmospheric Chemistry and Physics, 14, 6159–6176, https://doi.org/10.5194/acp-14-6159-2014, 2014.

Drinovec, L., Močnik, G., Zotter, P., Prévôt, A. S. H., Ruckstuhl, C., Coz, E., Rupakheti, M., Sciare, J., Müller, T., Wiedensohler, A., and Hansen, A. D. A.: The "dual-spot" Aethalometer: an improved measurement of aerosol black carbon with real-time loading compensation, Atmospheric Measurement Techniques, 8, 1965–1979, https://doi.org/10.5194/amt-8-1965-2015, publisher: Copernicus GmbH, 2015.

European Environment Agency, ed.: Europe's air quality status 2024, Publications Office, Luxembourg, ISBN 978-92-9480-650-5, https://doi.org/10.2800/5970, 2024.

European Topic Centre on Air pollution, transport, noise and industrial pollution, Colette, A., and Rouïl, L.: Air Quality Trends in Europe: 2000-2017, Eionet Report - ETC/ATNI 2019/16 ISBN 978-82-93752-15-8, 2020.

Ferranti, L., Corti, S., and Janousek, M.: Flow-dependent verification of the ECMWF ensemble over the Euro-Atlantic sector, Quarterly Journal of the Royal Meteorological Society, 141, 916–924, https://doi.org/10.1002/qj.2411, 2015.

Fomba, K. W., Müller, K., van Pinxteren, D., Poulain, L., van Pinxteren, M., and Herrmann, H.: Long-term chemical characterization of tropical and marine aerosols at the Cape Verde Atmospheric Observatory (CVAO) from 2007 to 2011, Atmospheric Chemistry and Physics, 14, 8883–8904, https://doi.org/10.5194/acp-14-8883-2014, 2014.

https://doi.org/10.5194/essd-2026-490
Preprint. Discussion started: 11 August 2026

Foret, G., Michoud, V., Kotthaus, S., Petit, J.-E., Baudic, A., Siour, G., Kim, Y., Doussin, J.-F., Dupont, J.-C., Formenti, P., Gaimoz, C., Ghersi, V., Gratien, A., Gros, V., Jaffrezo, J.-L., Haeffelin, M., Kreitz, M., Ravetta, F., Sartelet, K., Simon, L., Té, Y., Uzu, G., Zhang, S., Favez, O., and Beekmann, M.: The December 2016 extreme weather and particulate matter pollution episode in the Paris region (France), Atmospheric Environment, 291, 119 386, https://doi.org/10.1016/j.atmosenv.2022.119386, 2022.

Freney, E., Zhang, Y., Croteau, P., Amodeo, T., Williams, L., Truong, F., Petit, J.-E., Sciare, J., Sarda-Esteve, R., Bonnaire, N., Arumae, T., Aurela, M., Bougiatioti, A., Mihalopoulos, N., Coz, E., Artinano, B., Crenn, V., Elste, T., Heikkinen, L., Poulain, L., Wiedensohler, A., Herrmann, H., Priestman, M., Alastuey, A., Stavroulas, I., Tobler, A., Vasilescu, J., Zanca, N., Canagaratna, M., Carbone, C., Flentje, H., Green, D., Maasikmets, M., Marmureanu, L., Minguillon, M. C., Prevot, A. S. H., Gros, V., Jayne, J., and Favez, O.: The second ACTRIS inter-comparison (2016) for Aerosol Chemical Speciation Monitors (ACSM): Calibration protocols and instrument performance evaluations, Aerosol Science and Technology, 53, 830–842, https://doi.org/10.1080/02786826.2019.1608901, 2019.

Grams, C. M.: A life cycle definition of year-round weather regimes in the North Atlantic European region, https://doi.org/10.5194/egusphere-2025-6385, 2026.

Haeffelin, M., Barthès, L., Bock, O., Boitel, C., Bony, S., Bouniol, D., Chepfer, H., Chiriaco, M., Cuesta, J., Delanoë, J., Drobinski, P., Dufresne, J.-L., Flamant, C., Grall, M., Hodzic, A., Hourdin, F., Lapouge, F., Lemaître, Y., Mathieu, A., Morille, Y., Naud, C., Noël, V., O'Hirok, W., Pelon, J., Pietras, C., Protat, A., Romand, B., Scialom, G., and Vautard, R.: SIRTA, a ground-based atmospheric observatory for cloud and aerosol research, Annales Geophysicae, 23, 253–275, https://doi.org/10.5194/angeo-23-253-2005, 2005.

Huang, R.-J., Li, Y. J., Chen, Q., Zhang, Y., Lin, C., Chan, C. K., Yu, J. Z., De Gouw, J., Tong, S., Jiang, J., Wang, W., Ding, X., Wang, X., Ge, M., Zhou, W., Worsnop, D., Boy, M., Bilde, M., Dusek, U., Carlton, A. G., Hoffmann, T., McNeill, V. F., and Glasius, M.: Secondary organic aerosol in urban China: A distinct chemical regime for air pollution studies, Science, 389, eadq2840, https://doi.org/10.1126/science.adq2840, 2025.

Hussain, M. and Mahmud, I.: pyMannKendall: a python package for non parametric Mann Kendall family of trend tests., Journal of Open Source Software, 4, 1556, https://doi.org/10.21105/joss.01556, 2019.

Jayne, J. T., Leard, D. C., Zhang, X., Davidovits, P., Smith, K. A., Kolb, C. E., and Worsnop, D. R.: Development of an Aerosol Mass Spectrometer for Size and Composition Analysis of Submicron Particles, Aerosol Science and Technology, 33, 49–70, https://doi.org/10.1080/027868200410840, 2000.

Jones, P. D. and Lister, D. H.: The influence of the circulation on surface temperature and precipitation patterns over Europe, Climate of the Past, 5, 259–267, https://doi.org/10.5194/cp-5-259-2009, 2009.

Klopper, D., Formenti, P., Namwoonde, A., Cazaunau, M., Chevaillier, S., Feron, A., Gaimoz, C., Hease, P., Lahmidi, F., Mirande-Bret, C., Triquet, S., Zeng, Z., and Piketh, S. J.: Chemical composition and source apportionment of atmospheric aerosols on the Namibian coast, Atmospheric Chemistry and Physics, 20, 15 811–15 833, https://doi.org/10.5194/acp-20-15811-2020, 2020.

Li, T., Yu, Y., Sun, Z., and Duan, J.: A comprehensive understanding of ambient particulate matter and its components on the adverse health effects based from epidemiological and laboratory evidence, Particle and Fibre Toxicology, 19, 67, https://doi.org/10.1186/s12989-022-00507-5, 2022.

Lolli, S.: Urban PM2.5 concentration monitoring: A review of recent advances in ground-based, satellite, model, and machine learning integration, Urban Climate, 63, 102 566, https://doi.org/10.1016/j.uclim.2025.102566, 2025.

Meng, Q., Zhang, Y., Zhong, S., Fang, J., Tang, L., Rao, Y., Zhou, M., Qiu, J., Xu, X., Petit, J.-E., Favez, O., and Ge, X.: Technical note: Reconstructing missing surface aerosol elemental carbon data in long-term series with ensemble learning, Atmospheric Chemistry and Physics, 25, 7485–7498, https://doi.org/10.5194/acp-25-7485-2025, 2025.

https://doi.org/10.5194/essd-2026-490
Preprint. Discussion started: 11 August 2026

Middlebrook, A. M., Bahreini, R., Jimenez, J. L., and Canagaratna, M. R.: Evaluation of Composition-Dependent Collection Efficiencies for the Aerodyne Aerosol Mass Spectrometer using Field Data, Aerosol Science and Technology, 46, 258–271, https://doi.org/10.1080/02786826.2011.620041, 2012.

Ng, N. L., Herndon, S. C., Trimborn, A., Canagaratna, M. R., Croteau, P. L., Onasch, T. B., Sueper, D., Worsnop, D. R., Zhang, Q., Sun, Y. L., and Jayne, J. T.: An Aerosol Chemical Speciation Monitor (ACSM) for Routine Monitoring of the Composition and Mass Concentrations of Ambient Aerosol, Aerosol Science and Technology, 45, 780–794, https://doi.org/10.1080/02786826.2011.560211, 2011.

Pandolfi, M., Alastuey, A., Pérez, N., Reche, C., Castro, I., Shatalov, V., and Querol, X.: Trends analysis of PM source contributions and chemical tracers in NE Spain during 2004–2014: a multi-exponential approach, Atmospheric Chemistry and Physics, 16, 11 787–11 805, https://doi.org/10.5194/acp-16-11787-2016, 2016.

Patel, K., Bhandari, S., Gani, S., Campmier, M. J., Kumar, P., Habib, G., Apte, J., and Hildebrandt Ruiz, L.: Sources and Dynamics of Submicron Aerosol during the Autumn Onset of the Air Pollution Season in Delhi, India, ACS Earth and Space Chemistry, 5, 118–128, https://doi.org/10.1021/acsearthspacechem.0c00340, 2021.

Petit, J.-E., Favez, O., Sciare, J., Crenn, V., Sarda-Estève, R., Bonnaire, N., Močnik, G., Dupont, J.-C., Haeffelin, M., and Leoz-Garziandia, E.: Two years of near real-time chemical composition of submicron aerosols in the region of Paris using an Aerosol Chemical Speciation Monitor (ACSM) and a multi-wavelength Aethalometer, Atmospheric Chemistry and Physics, 15, 2985–3005, https://doi.org/10.5194/acp-15-2985-2015, 2015.

Petit, J.-E., Amodeo, T., Meleux, F., Bessagnet, B., Menut, L., Grenier, D., Pellan, Y., Ockler, A., Rocq, B., Gros, V., Sciare, J., and Favez, O.: Characterising an intense PM pollution episode in March 2015 in France from multi-site approach and near real time data: Climatology, variabilities, geographical origins and model evaluation, Atmospheric Environment, 155, 68–84, https://doi.org/10.1016/j.atmosenv.2017.02.012, 2017a.

Petit, J.-E., Favez, O., Albinet, A., and Canonaco, F.: A user-friendly tool for comprehensive evaluation of the geographical origins of atmospheric pollution: Wind and trajectory analyses, Environmental Modelling & Software, 88, 183–187, https://doi.org/10.1016/j.envsoft.2016.11.022, 2017b.

Petit, J.-E., Dupont, J.-C., Favez, O., Gros, V., Zhang, Y., Sciare, J., Simon, L., Truong, F., Bonnaire, N., Amodeo, T., Vautard, R., and Haeffelin, M.: Response of atmospheric composition to COVID-19 lockdown measures during spring in the Paris region (France), Atmospheric Chemistry and Physics, 21, 17 167–17 183, https://doi.org/10.5194/acp-21-17167-2021, 2021.

Petit, J.-E. and Brochet, J. and ACTRIS and GAW-WDCA: Measurement of Inorganics in air and particle phase at SIRTA Atmospheric Research Observatory, data hosted by EBAS at NILU, https://doi.org/10.48597/4RKH-6RDU, EBAS [dataset], 2025.

Pope, R. J., Savage, N. H., Chipperfield, M. P., Ordóñez, C., and Neal, L. S.: The influence of synoptic weather regimes on UK air quality: regional model studies of tropospheric column NO_2, Atmospheric Chemistry and Physics, 15, 11 201–11 215, https://doi.org/10.5194/acp-15-11201-2015, 2015.

Poulain, L., Spindler, G., Grüner, A., Tuch, T., Stieger, B., Van Pinxteren, D., Petit, J.-E., Favez, O., Herrmann, H., and Wiedensohler, A.: Multi-year ACSM measurements at the central European research station Melpitz (Germany) – Part 1: Instrument robustness, quality assurance, and impact of upper size cutoff diameter, Atmospheric Measurement Techniques, 13, 4973–4994, https://doi.org/10.5194/amt-13-4973-2020, 2020.

Ramonet, M. and Bouillon, L.: Ten years of measurements (2012-2022) of the atmospheric composition at Saclay/SIRTA Observatory in the Ile de France Region as part of ICOS and ACTRIS, https://doi.org/10.57932/5c399263-a317-41b7-8900-184b177c4216, [dataset], 2025.

https://doi.org/10.5194/essd-2026-490
Preprint. Discussion started: 11 August 2026

Savadkoohi, M., Pandolfi, M., Favez, O., Putaud, J.-P., Eleftheriadis, K., Fiebig, M., Hopke, P. K., Laj, P., Wiedensohler, A., Alados-Arboledas, L., Bastian, S., Chazeau, B., María, C., Colombi, C., Costabile, F., Green, D. C., Hueglin, C., Liakakou, E., Luoma, K., Listrani, S., Mihalopoulos, N., Marchand, N., Močnik, G., Niemi, J. V., Ondráček, J., Petit, J.-E., Rattigan, O. V., Reche, C., Timonen, H., Titos, G., Tremper, A. H., Vratolis, S., Vodička, P., Funes, E. Y., Zíková, N., Harrison, R. M., Petäjä, T., Alastuey, A., and Querol, X.: Recommendations for reporting equivalent black carbon (eBC) mass concentrations based on long-term pan-European in-situ observations, Environment International, 185, 108 553, https://doi.org/10.1016/j.envint.2024.108553, 2024.

Schneider, M. Y., Jiang, J., Chen, Y., Aas, W., Atabakhsh, S., Aurela, M., Belis, C., Bougiatioti, A., Bressi, M., Canonaco, F., Chazeau, B., Chebaicheb, H., Ehn, M., Eleftheriadis, K., Favez, O., Flentje, H., Font, A., Freney, E., Gilardoni, S., Gini, M. I., Green, D. C., Heikkinen, L., Keernik, H., Lhotka, R., Lin, C., Maasikmets, M., Marchand, N., Minguillón, M. C., Necki, J., Ovadnevaite, J., Paglione, M., Pauraite, J., Petit, J.-E., Pikridas, M., Platt, S., Pokorná, P., Poluzzi, V., Poulain, L., Riffault, V., Rinaldi, M., Sciare, J., Sosedova, Y., Stavroulas, I., Timonen, H., Tobler, A., Vasilescu, J., Via, M., Vodička, P., Zhang, Y., Zografou, O., Daellenbach, K. R., Upadhyay, A., Chen, G. I., Manousakas, M.-I., El Haddad, I., and Prévôt, A. S.: Analysis of source regions and transport pathways of sub-micron aerosol components in Europe, Environmental Pollution, 385, 127 110, https://doi.org/10.1016/j.envpol.2025.127110, 2025.

Stein, A. F., Draxler, R. R., Rolph, G. D., Stunder, B. J. B., Cohen, M. D., and Ngan, F.: NOAA's HYSPLIT Atmospheric Transport and Dispersion Modeling System, Bulletin of the American Meteorological Society, 96, 2059–2077, https://doi.org/10.1175/BAMS-D-14-00110.1, 2015.

Stirnberg, R., Cermak, J., Kotthaus, S., Haeffelin, M., Andersen, H., Fuchs, J., Kim, M., Petit, J.-E., and Favez, O.: Meteorology-driven variability of air pollution (PM_1) revealed with explainable machine learning, Atmospheric Chemistry and Physics, 21, 3919–3948, https://doi.org/10.5194/acp-21-3919-2021, 2021.

Szopa, S., Naik, V., Adhikary, B., Artaxo, P., Berntsen, T., Collins, W., Fuzzi, S., Gallardo, L., Kiendler-Scharr, A., Klimont, Z., Liao, H., Unger, N., and Zanis, P.: Climate Change 2021 – The Physical Science Basis Working Group I Contribution to the Sixth Assessment Report of the Intergovernmental Panel on Climate Change , pp. 817 - 922, Cambridge University Press, 1 edn., ISBN 978-1-009-15789-6, https://doi.org/10.1017/9781009157896.008, 2023.

Tørseth, K., Aas, W., Breivik, K., Fjæraa, A. M., Fiebig, M., Hjellbrekke, A. G., Lund Myhre, C., Solberg, S., and Yttri, K. E.: Introduction to the European Monitoring and Evaluation Programme (EMEP) and observed atmospheric composition change during 1972ndash;2009, Atmospheric Chemistry and Physics, 12, 5447–5481, https://doi.org/10.5194/acp-12-5447-2012, 2012.

Tsimpidi, A. P., Scholz, S. M. C., Milousis, A., Mihalopoulos, N., and Karydis, V. A.: Aerosol composition trends during 2000–2020: in-depth insights from model predictions and multiple worldwide near-surface observation datasets, Atmospheric Chemistry and Physics, 25, 10 183–10 213, https://doi.org/10.5194/acp-25-10183-2025, 2025.

Tsyro, S., Aas, W., Colette, A., Andersson, C., Bessagnet, B., Ciarelli, G., Couvidat, F., Cuvelier, K., Manders, A., Mar, K., Mircea, M., Otero, N., Pay, M.-T., Raffort, V., Roustan, Y., Theobald, M. R., Vivanco, M. G., Fagerli, H., Wind, P., Briganti, G., Cappelletti, A., D'Isidoro, M., and Adani, M.: Eurodelta multi-model simulated and observed particulate matter trends in Europe in the period of 1990–2010, Atmospheric Chemistry and Physics, 22, 7207–7257, https://doi.org/10.5194/acp-22-7207-2022, 2022.

WHO: WHO global air quality guidelines: particulate matter (PM2.5 and PM10), ozone, nitrogen dioxide, sulfur dioxide and carbon monoxide, WHO European Centre for Environment and Health, Bonn, Germany, ISBN 978-92-4-003422-8, oCLC: 1285551052, 2021.

WMO and GAW: WMO/GAW Aerosol Measurement Procedures, Guidelines and Recommendations, Tech. Rep. 227, World Meteorological Organization and Global Atmosphere Watch, ISBN 978-92-63-11177-7, 2016.

https://doi.org/10.5194/essd-2026-490
Preprint. Discussion started: 11 August 2026

Zhang, J. K., Sun, Y., Liu, Z. R., Ji, D. S., Hu, B., Liu, Q., and Wang, Y. S.: Characterization of submicron aerosols during a month of serious pollution in Beijing, 2013, Atmospheric Chemistry and Physics, 14, 2887–2903, https://doi.org/10.5194/acp-14-2887-2014, 2014.

Zhang, Y., Favez, O., Petit, J.-E., Canonaco, F., Truong, F., Bonnaire, N., Crenn, V., Amodeo, T., Prévôt, A. S. H., Sciare, J., Gros, V., and Albinet, A.: Six-year source apportionment of submicron organic aerosols from near-continuous highly time-resolved measurements at SIRTA (Paris area, France), Atmospheric Chemistry and Physics, 19, 14 755–14 776, https://doi.org/10.5194/acp-19-14755-2019, 2019.

Zhou, W., Xu, W., Kim, H., Zhang, Q., Fu, P., Worsnop, D. R., and Sun, Y.: A review of aerosol chemistry in Asia: insights from aerosol mass spectrometer measurements, Environmental Science: Processes & Impacts, 22, 1616–1653, https://doi.org/10.1039/D0EM00212G, 2020.